Structural Tolerances of Optical Characteristics in Various types of Photonic Lattices

Stanislav KRAUS, Michal LUCKI

Department of Telecommunications Engineering, Faculty of Electrical Engineering,
Czech Technical University in Prague, Technicka 2, 166 27 Prague, Czech Republic

stanislav.kraus@fel.cvut.cz, lucki@fel.cvut.cz

Abstract. *A systematic study of various photonic crystal lattices and their optical characteristics is carried out in this paper. Sensitivity of both dispersion and effective mode area characteristics to deviations of particular structural parameters of the lattices are the main studied topics. The presented results can be exploited during the design of fibers and new devices utilizing the studied lattices, when strict requirements on optical characteristics of the fabricated devices are imposed. Performance benefits for the implementation of particular lattices types in photonic designs are shown.*

Keywords

Dispersion, effective more area, FDFD, photonic lattice, tolerance.

1. Introduction

Photonic crystals fibers (PCFs) exhibit two-dimensional periodicity in a cross-section compared to traditional rotational symmetry. Dispersion profile of PCFs can be tailored for desired applications ranging from dispersion compensation [1] to non-linear optics [2]. Another distinctive advantage of a PCF over conventional fibers includes ability to achieve very small effective mode area for non-linear applications as well as large effective mode areas while maintaining unique single mode operation. A typical high-index guiding PCF structure consists of a solid core made of host material (typically silica glass), surrounded by cladding, and formed by the composition of multiple air holes along the fiber in the host material. These air holes are arranged in a periodic lattice and prevent light from escaping from the solid core. The high-index guiding mechanism is known as modified total internal reflection (M-TIR), [3]. Since lattice determines dimensions and shape of the core, it significantly influences the effective mode area and birefringence. Geometry of a photonic lattice and the shape of holes affect dispersion, particularly its waveguide portion, since the lattice determines the field distribution of guided modes within the structure.

In this paper, the characteristics of photonic crystal lattices are discussed from the viewpoint of structural tolerances of dispersion and effective mode area. The outline of particular lattice types for their potential implementation in photonic designs is included.

2. State of the Art

The early designs of PCFs [4] utilized hexagonal lattice, still used in recent designs [5], [6], [7], although certain modifications of the hexagonal lattice for achieving desired properties, e.g. large mode area (larger than 80 μm^2) by insertion of core defects, are known [5]. The hexagonal lattice is attractive owing to its simplicity, since few design parameters is responsible for the lattice properties. Furthermore, the hexagonal layout of capillaries ensures that pressure among capillaries during the drawing process is applied omni-directionally, thus preventing the transformation into different layout. The idea of stronger confinement of light within a core led to an increase in number of air holes within rings. This approach was utilized in [8], [9], where an octagonal lattice was proposed and also in [10], where the number of air holes within the first ring was even increased to ten, creating a decagonal lattice. The main benefits sourcing from the stronger confinement of light are the lower confinement loss and the wider range of wavelengths in the octagonal lattice compared to the hexagonal lattice [8]. The decagonal lattice can provide high negative dispersion slope for PCF designs with small lattice pitch (being about 1 μm) and may be promising for non-linear optics as well, since the effective mode area as low as 2 μm^2 has already been reported [10]. Designs of PCFs with a square lattice were also proposed in many papers [11], [12], [13]. The results presented in [12] show lower

dispersion and lower dispersion slope for the square lattice than for the hexagonal lattice. This advantageous property was exploited to design a PCF for dispersion compensation from E to L wavelengths bands [12] or PCF for optical coherence tomography [13]. The achievement of the better control of effective mode area in PCFs was aimed in other proposals [14], [15], [16], which did not utilize the polygonal layout of air holes. On the other hand, in [15] and [16], the air holes form repeating equiangular spirals. The spiral is a geometrical arrangement that in many aspects resembles the form of a seashell. This allows controlling the optical characteristics by adjusting coefficients in exponential expressions of the spirals. In particular, very low effective mode area of 0.71 μm^2 [15] is obtained, if the spirals are tightly curled. Nevertheless, the repeatable fabrication of PCF deploying the equiangular spiral is still unresolved.

3. Material and Methods

The studied photonic lattices are comprised of silica glass as a background material and circular cladding air holes. This shape of holes is the most common in the generally accepted PCF designs and the most suitable for fabrication, since a preform is formed by stacking capillaries with a circular inner hole. In order to simplify and without restricting generality, the refractive index of air is considered as being constant and equal to 1 in the simulated wavelength range, whereas the dependence of refractive index upon wavelength for silica glass whose properties accounts for material dispersion, is modeled using the Sellmeier dispersive formula 1, [17]:

$$n^2 - 1 = \frac{0.6961663\lambda^2}{\lambda^2-(0.0684043)^2} + \frac{0.4079426\lambda^2}{\lambda^2-(0.1162414)^2} + \\ + \frac{0.8974794\lambda^2}{\lambda^2-(9.896161)^2}. \quad (1)$$

Three different photonic lattices are considered in simulations presented in this paper:

- hexagonal,
- square,
- octagonal.

These lattices can be easily described by a few geometrical parameters mentioned below. The considered lattices are optimized to support the fundamental mode only. In all the studied lattices, omitting the central air hole of the lattice forms the core. The basic forming unit of the hexagonal lattice is an equilateral triangle of air holes with diameter d, which has pitch Λ between adjacent air holes. The air holes with equidistance from the core center resemble hexagonal rings. The square lattice is obtained by repetition of the basic square unit with side length Λ. The octagonal lattice is formed by repeating an isosceles triangle of air holes with the vertex angle of 45° around the core center, which creates octagonal rings of air holes in the cladding, Fig. 1. The pitch between adjacent holes in the octagonal lattice is not uniform. The pitch between holes in adjacent rings is Λ, whereas the pitch between the adjacent holes in the same ring is $\Lambda_1 \cong 0.765\Lambda$. The diameter of the core is equal to $2\Lambda - d$ for all the studied lattices. The reference values of parameters are summarized in Tab. 1. The selection of reference values should ensure that trends in characteristics can be rescaled for other values of the parameters, if the ratio d/Λ is unchanged, and the optical characteristics fit within their linear region (i.e. results for a different set of parameters can be obtained by the shift of the reference characteristics).

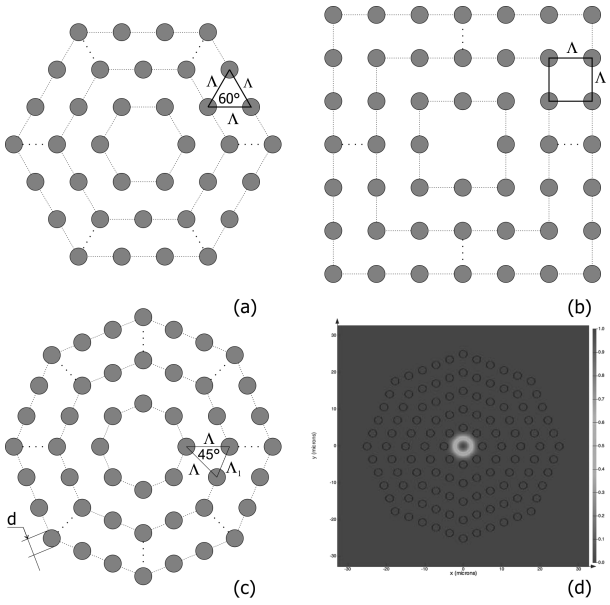

Fig. 1: Schematic of (a) hexagonal lattice, (b) square lattice, (c) octagonal lattice with denoted parameters, (d) optical mode profile within octagonal lattice.

Tab. 1: Reference design parameters of studied lattices.

pitch Λ [μm]	2
octagonal lattice - pitch Λ_1 [μm]	0.765Λ
air hole diameter d [μm]	2
number of rings N_r [−]	5
core diameter $2\Lambda - d$ [μm]	8

The results presented in this paper were obtained by using the full vectorial finite difference frequency domain method [18]. The meshing algorithm generates square mesh, which discretize the PCF structure, creating Yee computational cells. Alignment of field intensity vectors on edges and nodal positions within

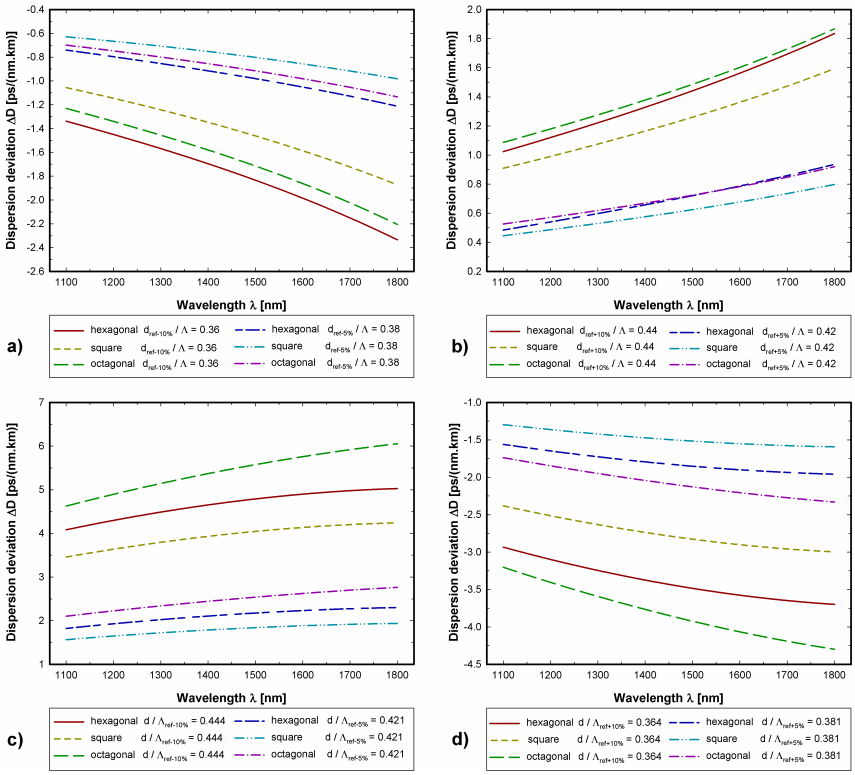

Fig. 2: Variation in chromatic dispersion with respect to wavelength for hexagonal, square and octagonal lattice for (a) −10 % decrease in diameter of air holes from the reference value, (b) +10 % increase in diameter of air holes from the reference value, (c) −10 % decrease in pitch from the reference value, (d) +10 % increase in pitch from the reference value.

each cell is chosen to satisfy continuity and boundary conditions between adjacent cells. Values of field intensity vectors are computed by employing approximation of Maxwell curl equations. Conformal mesh technique [19] is applied to the structure, where an interface between two materials is present within a computational cell. This improves the accuracy of the numerical solution, since Maxwell curl equations are computed along the material interface within the cell. Anisotropic perfectly matched layers (PMLs) [20] at the boundaries of the simulation region are utilized to model absorption of radiant energy from the simulation region. Utilization of PMLs at the edge of the simulation region satisfies the boundary conditions of Maxwell equations as well as reduces the necessary computational domain. Values of field intensity vectors are arranged in matrices, which enable to extract information about field profile and effective modal index n_{eff} of individual optical modes at different frequencies by solving these matrices.

The effective modal index is subsequently used to compute chromatic dispersion, which is the sum of material and waveguide dispersion. Dispersion is expressed using dispersion coefficient D [ps/(nm·km)], Eq. (2):

$$D = -\frac{1}{c}\frac{\partial^2 Re\{n_{eff}\}}{\partial\lambda^2}\frac{1}{L}, \tag{2}$$

where λ [nm] is wavelength, c [m·s^{-1}] is speed of light in vacuum, and L [km] is length of fiber. The quantitative assess of the transverse profile of the guided mode is expressed as an effective mode area A_{eff} [μm^2], Eq. (3), which is calculated based on the distribution of electric field intensity E [V·m^{-1}] within the structure:

$$A_{eff} = \frac{\left(\int\int |E|^2\, dxdy\right)^2}{\int\int |E|^4\, dxdy}. \tag{3}$$

The wavelength range considered in the simulations of lattice characteristics is 1100–1800 nm.

4. Results

Systematic study of wavelength-dependent variations in chromatic dispersion and in effective mode area of different photonic lattices with change in structural parameters is presented below. The absolute change in particular investigated parameter for 10 % and 5 % offset from the reference value of individual structural parameters is considered in the simulations. This corresponds to the independence of the considered geometrical parameters from the perspective of fabrication. The decision on the limit offset value would ensure that the

Tab. 2: Reference Values of Optical Characteristics.

Lattice	D [ps/(nm·km)] at 1550 nm	A_{eff} [μm^2] at 1550 nm	ZDW [nm]	DS [ps/(nm^2·km)]
Hexagonal	39.08	38.9	1148	<0.144
Square	36.25	47.9	1146	<0.131
Octagonal	42.02	31.7	1166	<0.134

results are valid for various fabrication methods, regardless of attainable precision of each method. The reference values of effective mode area, dispersion as well as zero dispersion wavelength (ZDW) and dispersion slope (DS) for the studied lattices are listed in Tab. 2. Dispersion characteristics of the studied lattices are evaluated first. Subsequently, the wavelength evolution of the effective mode area is studied.

First, the diameter of air holes is varied and the resulting change in chromatic dispersion is observed, Fig. 1(a), Fig. 1(b). It can be seen from the simulation results in Fig. 2(a), Fig. 2(b), that chromatic dispersion in the square lattice is the most immune to diameter changes of the air holes, where dispersion deviation is less than 1 ps/(nm·km) at the wavelength of 1200 nm. This is considered for the 10 % offset from the reference diameter. The curves of dispersion deviation for a hexagonal lattice and an octagonal lattice evolve in such a way that the difference in the first order derivations with respect to wavelength is slowly decreasing. The intersection point of the curve is laid beyond the studied wavelength range. The reason for this is similar arrangement of the air holes in n sided polygons in these lattices compared to a square lattice. Nevertheless, the hexagonal lattice exhibits the highest change in dispersion for negative deviation of air holes, in contrast to the octagonal lattice, whose highest change in dispersion for positive air holes diameter deviation is a fact.

The variation in pitch upon chromatic dispersion is depicted in Fig. 2(c), Fig. 2(d). It can be concluded that the square lattice is the most immune to deviation in pitch from all the studied lattices. Therefore, the square lattice can be perceived as suitable for photonic applications with a strict requirement for dispersion, such as wavelength conversion or four-wave mixing. A potential problem of the square lattice for its deployment in PCF may be more complicated fabrication. Unlike in the square lattice, high variation in chromatic dispersion in the octagonal lattice with change in both studied structural parameters is reported. This can be explained as being the result of a smaller distance between adjacent air holes within particular rings of the octagonal lattice compared to the hexagonal lattice or the square lattice. Therefore, change in diameter of the air holes or change in pitch, results in more significant change in waveguide dispersion, as a consequence of the change in field intensity in the vicinity of the boundary between the core and the cladding. Simulation results illustrated in Fig. 2(c) reveal that negative deviation of pitch alters dispersion characteristics for all the studied lattices more significantly. In addition, it can be concluded based on the comparison of Fig. 2(a) to Fig. 2(d) that the change in pitch affects chromatic dispersion of the studied lattices more than the change in diameter of the air holes. This property of lattices is related to change in core diameter, which is more prone to pitch deviation and less to the holes. Regardless of the lattice type, change in dispersion characteristics due to change in studied structural parameters is more of concern for long wavelength region.

The results on variation in effective mode area upon wavelength are depicted in Fig. 3. Proper design recommendations are provided based on the generalized characteristics of effective mode area of the studied lattices. For instance, negative deviation of air holes should be avoided during fabrication, since it alters the value of effective mode area (Fig. 3(a), Fig. 2(b)) more significantly, compared to enlargement of air holes. Deviation of pitch is more of concern for change in effective mode area than deviation of air holes, which can be inferred from Fig. 3. This can be attributed to higher sensitivity of the core size to variation in pitch rather than to variation in diameter of air holes. Moreover, the results reveal that the studied lattices are more prone to positive deviation in pitch. This finding demonstrates the octagonal lattice, for which the 10 % negative (resp. positive) deviation of pitch changes the effective mode area at 1500 nm by -7.4 μm^2 (resp. 8.7 μm^2). The effective mode area of octagonal lattice is the most insensitive to variation in both pitch and air hole diameter, which is caused by strong confinement (low value of A_{eff}) of the fundamental mode -98.5 % of power of the fundamental mode is located in the core, whereas only 94.3 % and 93.8 % of power is located in the same area for the hexagonal and the square lattice respectively. Changes in structural parameters affect the effective mode area mostly at long wavelengths (Fig. 3), since the electromagnetic field spreads more toward cladding with increase in wavelength. It is also noteworthy to mention that the wavelength dependence of variation in effective mode area is near-linear in the considered wavelength range, except for negative deviation of air holes in the hexagonal lat-

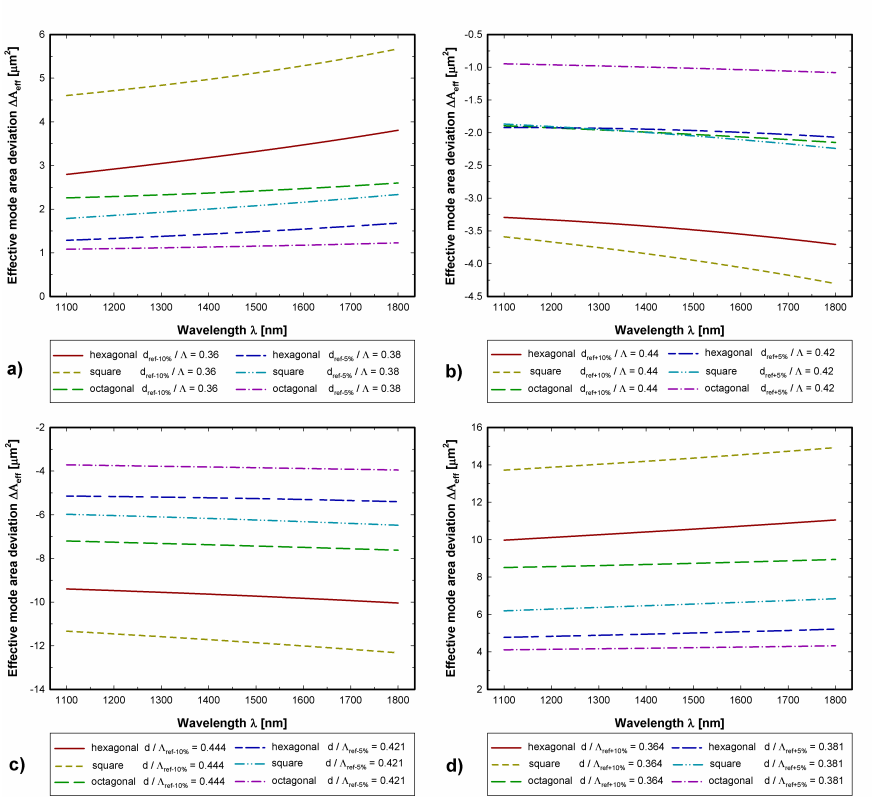

Fig. 3: Wavelength dependent variance in effective mode area for hexagonal, square and octagonal lattice for (a) −10 % decrease in diameter of air holes from the reference value, (b) +10 % increase in diameter of air holes from the reference value, (c) −10 % decrease in pitch from the reference value, (d) +10 % increase in pitch from the reference value.

tice Fig. 3(a). Hence, it is possible to predict a change in effective mode area of PCFs utilizing the studied lattices, if readjustment of the operating wavelength is required.

5. Conclusion

Different photonic lattices were investigated from the perspective of their structural parameters. Potential PCFs deploying the studied lattices should be designed to avoid variation in pitch, which predominantly influences characteristics of both chromatic dispersion and effective mode area. The highest insensitivity of chromatic dispersion to change in structural parameters is found for the square lattice. The utilization of the octagonal lattice is promising for applications requiring low variation in effective mode area, such as high power fiber lasers. For such applications one has to consider a lattice different from the hexagonal carefully. The main contribution of this paper is the presented sensitivity study of optical characteristics to structural deviations, which should be taken into account in future PCFs designs, especially those with non hexagonal lattice.

Acknowledgment

This work has been supported by the CTU grant under project SGS13/201/OHK3/3T/13.

References

[1] NAKAJIMA, K., T. MATSUI, K. KUROKAWA, K. TAJIMA and I. SANKAWA. High-Speed and Wideband Transmission Using Dispersion-Compensating/Managing Photonic Crystal Fiber and Dispersion-Shifted Fiber. *Journal of Lightwave Technology*. 2007, vol. 25, iss. 9, pp. 2719–2726. ISSN 0733-8724. DOI: 10.1109/JLT.2007.902754.

[2] SHASHIDHARAN, S., J. JOHNY, S. K. SUDHEER and K. S. KUMAR. Design and Simulation of Non Linear Photonic Crystal Fiber for Supercontinuum Generation and Its Application in Optical Coherence Tomography. In: *Symposium on Photonics and Optoelectronics*. Shanghai: IEEE, 2012, pp. 1–4. ISBN 978-1-4577-0909-8. DOI: 10.1109/SOPO.2012.6271023.

[3] BROENG, J., D. MOGILEVSTEV, S. E. BARKOU and A. BJARKLEV. Photonic Crystal Fibers: A New Class of Optical Waveguides. *Optical Fiber Technology*. 1999, vol. 5, iss. 3, pp. 305–330. ISSN 1068-5200. DOI: 10.1006/ofte.1998.0279.

[4] KNIGHT, J. C., T. A. BIRKS, P. St. J. RUSSELL and D. M. ATKIN. All-silica single-mode optical fiber with photonic crystal cladding. *Optics Letters*. 1996, vol. 21, iss. 19, pp. 1547–1549. ISSN 0146-9592. DOI: 10.1364/OL.21.001547.

[5] ROSTAMI, A. and H. SOOFI. Correspondence Between Effective Mode Area and Dispersion Variations in Defected Core Photonic Crystal Fibers. *Journal of Lightwave Technology*. 2011, vol. 29, iss. 2, pp. 234–241. ISSN 0733-8724. DOI: 10.1109/JLT.2010.2100808.

[6] LUCKI, M. Optimization of microstructured fiber for dispersion compensation purposes. In: *International Conference on Transparent Optical Networks*. Stockholm: IEEE, 2011, pp. 1–4. ISBN 978-1-4577-0881-7. DOI: 10.1109/ICTON.2011.5971024.

[7] LUCKI, M., R. ZELENY, K. KALLI, J. KANKA and A. MENDEZ. Broadband submicron flattened dispersion compensating fiber with asymmetrical fluoride doped core. In: *Micro-structured and Specialty Optical Fibres II*. Bellingham: SPIE, 2013, 87750M-1–87750M-8. ISBN 978-0-8194-9577-8. DOI: 10.1117/12.2017554.

[8] CHIANG, J.-S. and T.-L. WU. Analysis of propagation characteristics for an octagonal photonic crystal fiber (O-PCF). *Optics Communications*. 2006, vol. 258, iss. 2, pp. 170–176. ISSN 0030-4018. DOI: 10.1016/j.optcom.

[9] NEJAD, Sh. Mohammad, M. ALIRAMEZANI and M. POURMAHYABADI. Novel Design of an Octagonal Photonic Crystal Fiber with Ultra-Flattened Dispersion and Ultra-Low Loss. In: *International Conference on Broadband Communications, Information Technology*. Gauteng: IEEE, 2008, pp. 221–226. ISBN 978-1-4244-3281-3. DOI: 10.1109/BROADCOM.2008.12.

[10] RAZZAK, S. M. A., Y. NAMIHIRA, M. A. G. KHAN, F. BEGUM and S. KAIJAGE. Chromatic Dispersion Properties of A Decagonal Photonic Crystal Fiber. In: *International Conference on Information and Communication Technology*. Dhaka: IEEE, 2007, pp. 159–162. ISBN 984-32-3394-8. DOI: 10.1109/ICICT.2007.375365.

[11] ROJA, M. M. and R. K. SHEVGAONKAR. Geometrical Parameters Identification for Zero Dispersion in Square Lattice Photonic Crystal Fiber using Contour Plots. In: *International Conference on Signal Processing, Communications and Networking*. Chennai: IEEE, 2008, pp. 116–118. ISBN 978-1-4244-1924-1. DOI: 10.1109/ICSCN.2008.4447172.

[12] NEJAD, S. M. and N. EHTESHAMI. A novel design to compensate dispersion for square-lattice photonic crystal fiber over E to L wavelength bands. In: *International Symposium on Communication Systems Networks and Digital Signal Processing*. Newcastle: IEEE, 2010, pp. 654–658. ISBN 978-1-86135-369-6.

[13] NAMIHIRA, Y., M. A. HOSSAIN, J. LIU, T. KOGA, T. KINJO, Y. HIRAKO, F. BEGUM, S. F. KAIJAGE, S. M. A. RAZZAK and S. NOZAKI. Dispersion flattened nonlinear square photonic crystal fiber for dental OCT. In: *International Conference on Communication Technology and Application*. Beijing: IET, 2011, pp. 819–823. ISBN 978-1-61839-926-7. DOI: 10.1049/cp.2011.0783.

[14] RAZZAK, S. M. A., Y. NAMIHIRA, M. A. G KHAN, M. S. ANOWER and N. H. HAI. Transmission Characteristics of Circular Ring PCF and Octagonal PCF: A Comparison. In: *International Conference on Electrical and Computer Engineering*. Dhaka: IEEE, 2006, pp. 266–269. ISBN 98432-3814-1. DOI: 10.1109/ICECE.2006.355623.

[15] AGRAWAL, A., N. KEJALAKSHMY, B. M. A. RAHMAN and K. T. V. GRATTAN. Soft Glass Equiangular Spiral Photonic Crystal Fiber for Supercontinuum Generation. *Photonics Technology Letters*. 2009, vol. 21, iss. 22, pp. 1722–1724. ISSN 1041-1135. DOI: 10.1109/LPT.2009.2032523.

[16] HASAN, D. M. N., M. N. HOSSAIN, K. M. MOHSIN and M. S. ALAM. Optical characterization of a chalcogenide glass nanophotonic device. In: *International Technical Conference TENCON*. Fukuoka: IEEE, 2010, pp. 1915–1920. ISBN 978-1-4244-6889-8. DOI: 10.1109/TENCON.2010.5686431.

[17] BASS, M. *Handbook of Optics: Optical Properties of Materials, Nonlinear Optics, Quantum Optics*. New York: McGraw-Hill Education, 2009. ISBN 978-0-07-149892-0.

[18] ZHU, Z. and T. BROWN. Full-vectorial finite-difference analysis of microstructured optical fibers. *Optics Express*. 2002, vol. 10, iss. 17, pp. 853–864. ISSN 1094-4087. DOI: 10.1364/OE.10.000853.

[19] WENHUA Y. and R. MITTRA. A conformal finite difference time domain technique

for modeling curved dielectric surfaces. *Microwave and Wireless Components Letters*. 2001, vol. 11, iss. 1, pp. 25–27. ISSN 1531-1309. DOI: 10.1109/7260.905957.

[20] TAFLOVE, A. and S. C. HAGNESS. *Computational electrodynamics: the finite-difference time-domain method*. Boston: Artech House, 2005. ISBN 15-805-3832-0.

About Authors

Stanislav KRAUS was born in 1986. He received his M.Sc. in electrical engineering from the Czech Technical University in Prague in 2011. His research interests include design of optical photonic structures and optical communication systems.

Michal LUCKI received his Ph.D. from the Czech Technical University in Prague in 2007. His research interests include photonics, optoelectronics, material engineering and solid state physics. He is now a team leader and an investigator of a few grant projects focused on Photonic Crystal Fibers, among others.